Open Access

Recent Progress in Materials

LIDSEN Publishing Inc.

Original Research

Reaction Kinetics and Characterization of Slag-Based, High Strength, "Just-Add-Water" Type (One-Part) Alkali-Activated Binders

Akash Dakhane [†, ‡], Narayanan Neithalath [†, *]

School of Sustainable Engineering and the Built Environment, Arizona State University, Tempe AZ, USA; E-Mails: adakhane@asu.edu; Narayanan.Neithalath@asu.edu

‡ Current Affiliation: Intel Corporation, Hilsboro, OR, USA

† These authors contributed equally to this work.

* **Correspondence:** Narayanan Neithalath; E-Mail: Narayanan.Neithalath@asu.edu

Academic Editor: Mazen Alshaaer

Special Issue: Synthesis, Characterisation, and Applications of Functional Geopolymeric Materials

Recent Progress in Materials
2022, volume 4, issue 2
doi:10.21926/rpm.2202006

Received: February 03, 2022
Accepted: April 05, 2022
Published: April 08, 2022

Abstract

The influence of different levels of alkalinity, expressed using M_2O-to-binder ratio (n) and activator SiO_2-to-M_2O ratio (M_s), (M being the Na^+ or K^+ cation) on the reaction kinetics, compressive strength development and the reaction product formation in slag-based systems activated using alkali powders are discussed. The fundamental idea is to better understand one-part, "just-add-water" type alkali activated binders that are easy-to-use than the systems that rely on liquid activators. The difference in the behavior of the systems with changes in the cationic species (Na^+ or K^+) and the overall levels of alkalinity is elucidated. Heat release and its rate, and thermal analysis and Fourier Transform Infrared Spectroscopy (FTIR) are used for the characterization of the reaction and the products formed. The influence of activator alkalinity on the initial dissolution and acceleration phases is examined using isothermal calorimetry. An increase in M_s is found to result in reduced early-age and slightly increased later-age compressive strengths. The activator cationic species influences later-age strengths, with K-silicate activated mortars showing a higher strength. The strength data is related to the

C-(A)-S-H gel formation. The study shows that slag-based binders can be proportioned to obtained compressive strengths in excess of 80 MPa at later ages (56 days), and up to 30 MPa within 72 hours. The optimal alkali levels based on n and M_s for both the Na- and K-based activator systems are determined.

Keywords
Slag activation; powder activator; compressive strength; heat of reaction; C-(A)-S-H gel

1. Introduction

The adverse effects of CO_2 emission and energy demand of ordinary portland cement (OPC) production have fueled the search for sustainable substitutes for a long time [1]. Several partial cement replacement materials have broken through in the recent past - in addition to established partial cement substitutes such as fly ash and ground granulated blast furnace slag, materials such as ground limestone are increasingly becoming a part of mainstream concretes. However, extension of partial cement substitution to total cement replacement can only be accomplished through the activation of aluminosilicate materials such as fly ash and slag with concentrated alkalis. Alkali activation is an efficient method to produce for sustainable binders for concrete construction, since the use of waste or by-product materials as the source materials result in significant reductions in carbon and energy impacts [2-7]. While the concept, mechanisms, reaction effects, and properties of alkali activated binders are well known, concern on the use of corrosive alkaline activators, and in some cases, the need for elevated temperature curing, have resulted in these systems not being widely used in practice. A large number of research studies have appeared in the literature over the past couple of decades, and it is generally understood that such binders can be proportioned to have comparable or better mechanical and durability characteristics as that of conventional OPC concretes [7-12].These properties are inherently linked to the reaction product characteristics which are dependent on the physico-chemical characteristics of the source materials, activators, and the type of curing [13-15].

When a calcium-rich source material is activated by an alkaline solution, the poly-condensation reactions produce poorly crystalline C-A-S-H or C-M-A-S-H (where M is Na or K) gels as the reaction product. The higher levels of alkalinity in these systems results in breaking of the silicate bonds in slag which are then repolymerized to incorporate Al into the silica structure. The C/S ratios in the reaction products of alkali activated slags are reported to lower than those in conventional OPC systems [16]. Differences exist in the reaction product constitution when different alkaline activators are used. The differences could be because of the cationic type of the activator, activator alkalinity, or the ratio of silica-to-alkali oxide in the activator.

Generally, an activator solution - sodium or potassium silicates and/or hydroxides, is used as the activator, which is then mixed with precursor solids – commonly, slag or fly ash. It is also possible that the activator can be in a powder form, and can be pre-blended with the source material, so that “just-add-water” type binder systems can be formulated [17-19]. In fact, from a commercial standpoint, such blends are attractive for applications such as grouts, sealants, and repair products, in addition to conventional construction applications. Moreover, this approach can eliminate the

issues associated with the use of corrosive and hazardous activator solutions, that have hindered the use of alkali-activated binders to a great extent. However the use of one-part binders are also not without pitfalls - a main reason that one-part binders are not commonly used is the hygroscopic nature of the powders, even though a few studies report the use of such activators in laboratory experiments [20, 21]. The most common starting materials combination used in one-part alkali activated binder systems are fly ash and slag [22-24] sometimes with the starting materials being augmented with additional amorphous silica or alumina sources [25, 26] For a detailed review on the starting materials used in such systems, the readers are referred to [19]. The alkaline activators, in general, are powdered alkali hydroxides, silicates, carbonates or sulfates [24, 27]. For slag-based binders, CaO also has been proposed as an activator [28]. While admixtures such as ZnO and malic acid have been used to retard the setting of one-part alkali activated binders [29, 30], the results have not always been consistent.

This study attempts a comprehensive evaluation of the reaction kinetics, strength, and product formation in slags activated using both Na- and K-based alkali silicate/alkali hydroxide powders. The parameters that are considered in this work with respect to the activators include the influence of activator cation type (Na or K), total alkalinity provided by the activator (defined as the ratio of alkali oxide to the total source material content, referred to as *n*), and the molar ratio of silica-to-alkali oxide in the activator (M_s), which can be adjusted by the incorporation of hydroxides. Such a comprehensive treatment of the influence of alkali cationic type and activator concentrations is missing from the literature, especially towards the development of high-strength mixtures. The influence of all of the aforementioned parameters on: (a) the total rate and extent of reaction at early ages, (b) compressive strengths at early and later ages), and (c) reaction product formation are discussed in detail in this paper. The results reported here can be used to guide the development of alkali-activated binder products that only need the addition of water to set and harden in-place, similar to portland cements, but without the environmental impacts associated with portland cements.

2. Experimental Program

2.1 Materials and Mixture Proportioning

Ground granulated blast furnace slag (GGBFS) Type 100 conforming to ASTM C 989, having a chemical composition as shown in Table 1 is used as the source material in this study. The median particle size (d_{50}) of the slag is 8.9 μm as determined using dynamic light scattering.

Table 1 Chemical composition and physical properties of slag.

Chemical composition (% by mass)									Specific gravity	Specific surface area
SiO_2	Al_2O_3	Fe_2O_3	CaO	MgO	SO_3	Na_2O	K_2O	LOI		
36.0	10.5	0.67	39.8	7.93	2.10	0.27	0.80	3.01	2.90	487 m^2/kg

Two different powder activating agents were used to activate slag in this study: sodium silicate and potassium silicate. The following two parameters were considered in developing the mixture proportions: M_2O-to-slag (binder) ratio (*n*), and the silica modulus (SiO_2-to-M_2O ratio; mole-based) (M_s) of the activator [14, 31, 32]. The *n* value dictates the total amount of Na_2O or K_2O in the mixture,

which comes both from the Na- or K-silicates as well as the hydroxides added to provide a certain *n* value. The as-received sodium silicate powder used in this study has a molar M_s of 2.0 and the potassium silicate powder has a molar M_s of 2.5. The Na-silicate powder has a density of 0.73 g/cm^3 and a particle size distribution (PSD) with 97% passing through a 75 µm sieve, while the K-silicate powder has a density of 1.2, with 50% passing through a 75 µm sieve. For both the Na and K silicates, NaOH or KOH was added as necessary to bring the activator M_s down to 1.0 to 2.0 since beneficial strength development required M_s values in this range [14, 33]. The *n* values adopted in mixture proportioning ranged from 0.02 to 0.07. The water-to-powder ratio (w/p) in the range of 0.35 to 0.45 (mass-based) demonstrated sufficient workability for the alkali activated slag systems adopted using trial proportioning, and hence a value of 0.40 is used in this study. Table 2 summarizes the amount of activating agents required for 1000 g of slag, for an *n* value of 0.05 and the different M_s values used in this study. Note that only a very small amount of hydroxides were needed per 1000 g of slag, to obtain activator M_s value of 2.0, for an *n* of 0.05.

Table 2 Amounts of alkali silicate activators for *n* of 0.05, for 1000 g of slag.

Activator powder	Na-Si (M_s = 2.0)			K-Si (M_s = 2.5)		
Activator M_s	1	1.5	2	1	1.5	2
Na/K silicate powder(g)	72.58	108.9	145.2	51.86	77.79	103.7
NaOH/KOH (g)	33.30	17.69	2.08	35.81	23.93	12.04
Water (g)	431.9	445.1	458.2	427.0	435.3	443.6

For the compressive strength tests, mortars were prepared with a 45% sand volume fraction. The calculated amounts of slag, sand, and activating powders were first dry-mixed thoroughly in a laboratory mixer. The required amount of water was then added to the starting materials to prepare the mortars and mixed for approximately 2 minutes until a homogenous mixture is obtained. The mixtures were then cast in 50 mm cube molds for compressive testing and porosity measurements. The mortars were stored in the molds at 23 ± 1°C for 24 hours after which they were removed and stored in a moist chamber (23 ± 1°C, >98% RH) until the respective testing durations.

2.2 Test Methods

Isothermal calorimetry studies were carried out for 72 hours at a temperature of 25°C in accordance with ASTM C 1679 [34]. The activator powder and desired amount of water was initially mixed and allowed to cool down to ambient temperature. The solution was then added to the binder (slag) and the mixture placed in the calorimeter chamber. Direct addition of water to slag-activator powder blend was not adopted in this study for calorimetric studies because the reaction of alkalis with water release large amounts of heat immediately after mixing, which influences the heat release measurements using the isothermal calorimeter because of the sensitivity of the instrument. However, a previous study has shown that the early and later-age compressive strengths were independent of the methodology of activator addition (powder or liquid) as long as the proportions were the same [31]. The time elapsed between mixing and placing the mixture in the calorimeter was not more than 2 min [32]. The compressive strengths of three replicate 50 mm mortar cubes were determined in accordance with ASTM C 109 at ages of 1, 3, 14, 28 and 56 days of moist curing.

Thermo-gravimetric analysis (TGA) was performed on paste samples at ages of 1, 7, and 28 days using a Perkin Elmer simultaneous thermal analyzer (STA 6000). The sample was heated to 50^{o}C, held for 1 minute, and then heated to 1000^{o}C at a rate of 15^{o}C/min. An approximate quantification of the amount of C-(A)-S-H gel was attempted using the mass loss between 150^{o}C and 300^{o}C [35-37]. Fourier transform infrared (FTIR) spectroscopy was performed using a Genesis FTIR spectroscope augmented by an attenuated total reflection (ATR) attachment. FTIR spectroscopy was performed on samples at ages of 1, 7 and 28 days.

3. Results, Analysis and Discussions

3.1 Reaction Kinetics

The solubility of the activator powders in water has a significant influence on the early age reaction kinetics in "just-add-water" type systems. Activators with lower M_s or higher n have higher quantities of externally added alkali hydroxides, which result in reduction in the amounts of alkali silicate powder used. The silicate powder solubility, especially that of Na-silicate, decreases with an increase in the alkalinity of the solution (i.e., increasing alkali hydroxide powder addition). The solubility of the Na-silicate powder is lower than that of the K-silicate powder for the same n and M_s values, attributable to the fact that the hydration sphere of potassium ion is smaller [38-41]. This is because a greater number of solvent (i.e., water) molecules will be attracted by Na^+ owing to its larger charge-to-size ratio, thereby increasing the size of the hydration shell.

Figures 1(a) and (b) show the heat evolution rates of Na- and K-silicate powder activated slag pastes respectively, proportioned using an n value of 0.05 and M_s of 1, 1.5, and 2.0. The figures show two distinct peaks in the calorimetric curves, as a result of the reaction of slag with alkalis: an initial dissolution peak and a later acceleration peak. This is similar to the heat release signature of portland cement systems [42]. The initial peak noticed during the first few hours can be attributed to particle wetting and the dissolution of the slag particles in the highly alkaline medium [32, 42], attained through the dissolution of alkaline powders in water. The highly alkaline solution results in the rupture of the Ca-O, Al-O and Si-O bonds. Here, one needs to note that, since mixing between the slag and the activators was performed external to the calorimeter, the dissolution peak magnitudes may not be accurate; however they can be used for comparative purposes since all the experiments followed the same procedure [32]. At the lowest value of M_s (=1.0) for sodium silicate activators (Figure 1(a)), where there is a higher amount of hydroxides used (see Table 2), there is only one peak noted, which is characteristic of hydroxide activated slag systems [43]. This illustrates that the presence of silicate does not influence the hydration signature of alkali activated systems at lower values of M_s. As the M_s is increased (to 1.5 and 2.0), there is increased solubility of the silicates which is confirmed by the increased intensity and early occurrence of acceleration phase. The dormant period is reduced as the M_s is increased from 1.5 to 2.0. At an M_s of 2.0, the lower alkalinity enables faster dissolution of silicate powder, thereby facilitating the formation of C-A-S-H gel. Furthermore, with increasing M_s, the reducing alkalinity impedes the dissociation of the slag species, resulting in a reduced intensity of the acceleration peak. For the K-silicate activated system, some notable differences are observed as compared to the Na-based systems. Two peaks are noted in the hydration signature, irrespective of the activator alkalinity. Moreover, the times of occurrence of the acceleration peaks are delayed with increasing M_s. Since the solubility of K-silicate is higher than that of Na-silicate, even at higher alkalinities, there is the formation of C-A-S-H gel. In other

words, the influence of silicates is noted for all the values of activator parameters (*n* and M_s) studied here. The heat release signature follows a consistent trend with varying M_s values, contrary to the case for Na-silicates shown in Figure 1(a).

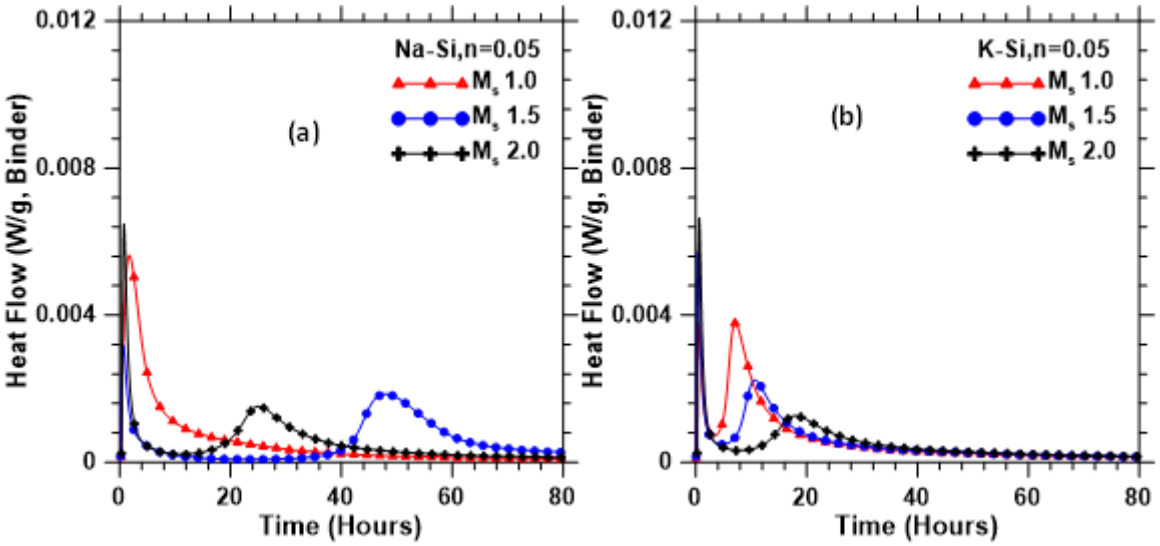

Figure 1 Heat evolution of slag pastes activated using activators of varying M_s from 1.0 to 2.0 (and a constant *n* of 0.05): (a) Na-silicate and (b) K-silicate at 25°C.

Figures 2(a) and Figures 2 (b) show the heat release rates for the sodium silicate activated pastes proportioned using two different activator M_s values and different *n* values. The *n* value was varied from 0.02 to 0.05 for an M_s of 1.5, and from 0.03 to 0.07 for an M_s of 2.0. The different *n* value ranges were used to ensure that, the combination of *n* and M_s provided a range of mixtures with similar alkalinity. Note that the alkalinity increases more with an increase in *n* value than with a decrease in M_s. For the Na-silicate activated mixtures, the acceleration peak is high at a lower *n* value for both M_s values, indicating the influence of the solubility of silicates, as discussed earlier. At a lower M_s value of 1.5 (Figure 2(a)), the acceleration peaks appear earlier for mixtures with lower *n* values, while the trends are reversed for an M_s of 2.0. In the former case, the total silica content in the mixture (given by the product of *n* and M_s) increases from 0.03 to 0.075 when *n* is increased from 0.02 to 0.05. Naturally, increase in silica content (and a consequent decrease in alkalinity) enhances the dormant period, and the acceleration period occurs later. However, when M_s is 2.0, the total silica content increases from 0.06 to 0.14 (double as that of the previous case) when *n* increases from 0.03 to 0.07. Note that the total alkalinity is also higher in this case, based on the *n* values used. Here, the very high silica contents require higher alkalinities to react faster, and thus the mixture with an *n* of 0.07 has the shortest dormant period. The magnitude of the acceleration peak is rather similar in both the cases.

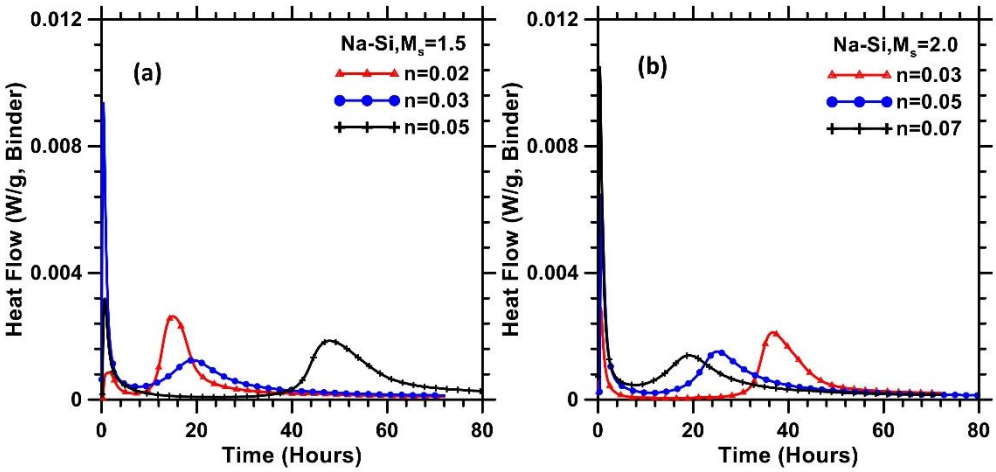

Figure 2 Heat evolution rate of slag pastes activated using Na-Silicate at M_s values of: (a) 1.5, and (b) 2.0, at different *n* values.

Figures 3(a) and (b) show the influence of activator concentration and silica modulus on the K-silicate activated pastes. Similar values were selected for the potassium silicate pastes as for the sodium silicate ones. For potassium silicate activated systems, it can be seen that there are insignificant differences in the heat release rates with changing *n* values (within the range considered) for both values of M_s used. Moreover, the dissolution peak is highly dependent on *n* value, the acceleration peak is independent of *n*. These observations can be explained rather easily – dissolution is dependent on alkalinity, but the formation of some products through the consumption of alkaline species is governed by rate of nucleation and growth. Given that the medium is super-saturated with the species that are to be precipitated, further higher levels of saturation makes no impact on the reaction kinetics.

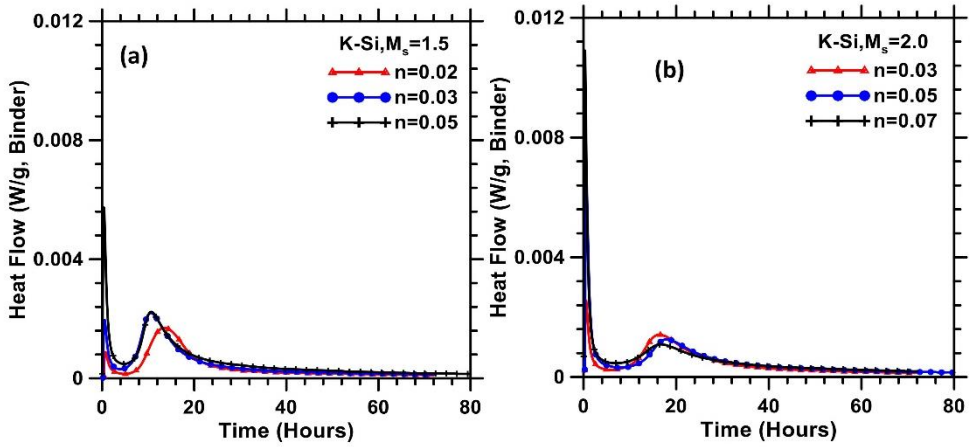

Figure 3 Heat evolution rate of slag pastes activated using K-Silicate at M_s values of: (a) 1.5, and (b) 2.0, at different *n* values.

Figures 4(a) and (b) show the cumulative heat release curves of Na- and K-silicate activated pastes proportioned using M_s values of 1.0, 1.5, and 2.0, and a constant *n* value of 0.05. Figure 4(a) shows that the longer dormant period, especially in high M_s pastes, for the Na-silicate activated slag

systems, results in a plateau region in the corresponding cumulative heat curves [14, 32]. As can be noticed from these figures, the cumulative heat at the end of 80 h is lower for the systems with a higher M_s (lower alkalinity), even though for the Na-silicate activated pastes, the paste with an M_s of 1.5 shows lower cumulative heats until close to 80 h, due to its lower dissolution peak. The cumulative heat-time relationship for the K-silicate based pastes are much more consistent with respect to the activator M_s as can be noticed from Figure 4(b). At the end of the test duration, the cumulative heat released is similar for the Na- and K-silicate activated pastes proportioned using the same activator M_s.

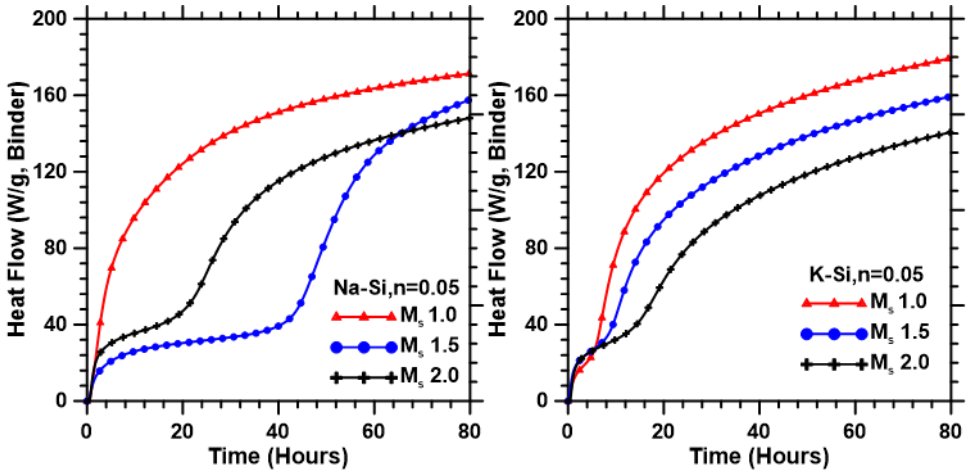

Figure 4 Cumulative heat release of slag pastes activated using: (a) Na-silicates and (b) K-silicates, for a of a constant *n* of 0.05 and different M_s values.

3.2 Compressive Strength and Its Development as a Function of Activator Concentration

The compressive strengths of sodium and potassium silicate activated mortars were determined after 1, 3, 14, 28 and 56 days of moist curing to understand the influence of the cationic species in the activator on the mechanical properties of the binder. The rate of strength development and the magnitude of the strength can be taken as an indication of the formation of the reaction product, C-(A)-S-H gel, in such systems. Figure 5 shows the strength development of slag mortars activated using Na- and K-silicates using activator M_s values ranging between 1.0 and 2.0, at a constant *n* value of 0.05. It can be immediately noticed that the strengths of the K-silicate activated systems are rather invariant with activator M_s, whereas there is significant difference in the strengths for Na-silicate activated mortars. This can be attributed, at least in part, to the enhanced solubility of K-silicates in alkaline solutions, resulting in *n* values being more dominant in dictating reaction product formation and strengths. In both cases, the higher later-age strengths are attained for mixtures that use a higher activator M_s, indicating the role of silicates in reaction product formation. It has been observed by the authors in previous studies that the strength of slag-based alkali activated mortars are higher when the activator contained silicates than when only hydroxide activators are used, even when the *n*-value is the same.

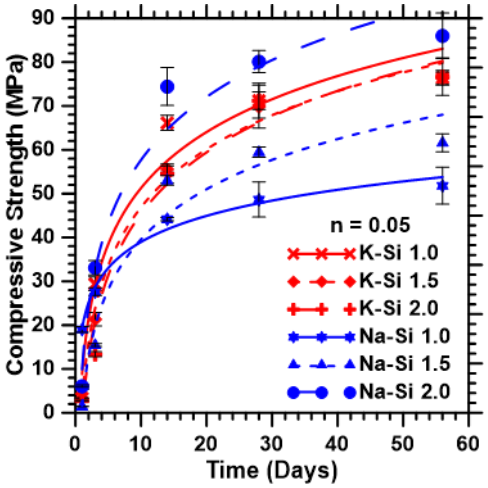

Figure 5 Compressive strength development of Na- and K-silicate activated slag mortars, with *n* of 0.05 varying *M.*

Figure 6 shows the influence of *n* values on the compressive strength development at two different activator M_s for both the Na- and K-silicate activated mortars. In all the cases, a higher *n* value results in higher strengths – more hydroxides available at higher *n* values allow for increased incorporation of Al into the gel structure. C-A-S-H gels with higher Al content demonstrate higher strengths. The scatter in the compressive strength results at all ages is lower at a higher M_s. Moreover, the influence of the cationic species – Na or K – is also less significant at higher values of M_s, irrespective of the total alkalinity denoted by the *n* value. The silicate species play a dominant role in reaction product formation and strength development in this case. Higher strengths are generally attained for the K-silicate activated mortars at higher *n* value, attributable to the better solubility of potassium silicate in alkaline media. The results show that 28 to 56 day compressive strengths of 50-80 MPa can be obtained through proper selection of the cationic species of the activator and alkalinity of the activation medium.

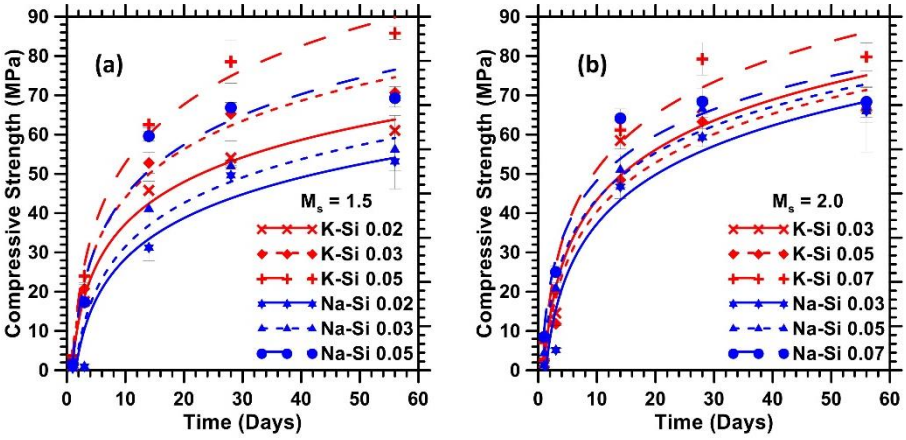

Figure 6 Compressive strength development of Na- and K-silicate activated mortars with varying *n* values and: (a) M_s of 1.5, and (b) M_s of 2.0.

Figure 7 presents the early-age (1- and 3-day) strengths of these systems as a function of the activator type, and chemical characteristics. Figure 7(a) illustrates the 1- and 3-day strengths of the

mortars made using Na- and K-silicates having an *n* value of 0.05 and different M_s values. It is noted that in general, an increase in M_s decreases the early age strengths, the reasons for which were explained earlier, and which can also be corroborated in association with the calorimetry results reported in the previous section. Up to 30 MPa compressive strengths are attained in 3 days. Even at 1-day, a highly alkaline Na-based activator system provides close to 20 MPa strength. At an M_s of 1.5, the enhancement in strength between 1 and 3 days is significant for the K-silicate activated systems. Figures 7(b) and (c) indicate the influence of *n* on the early-age compressive strength of these systems at activator M_s of 1.5 and 2.0 respectively. It is noted that increase in the *n* value typically results in an increase in the early-age compressive strength for both sodium and potassium based activation. The enhancement in strength between 1 and 3 days is higher for mortars made using a lower M_s value.

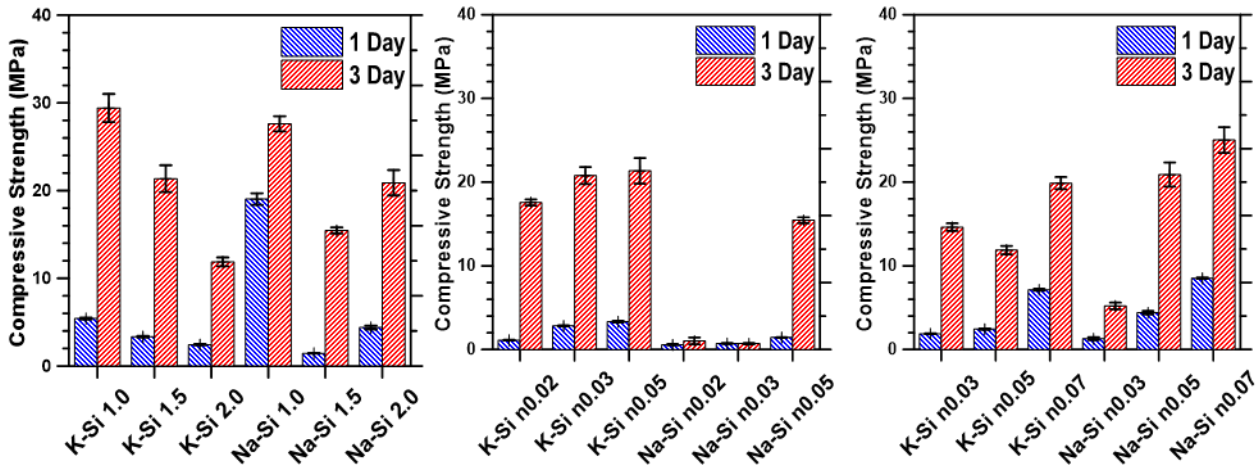

Figure 7 Early-age compressive strengths of Na- and K-silicate activated mortars with: (a) *n* of 0.05 varying M_s, (b) M_s of 1.5 varying *n* and (c) M_s of 2.0 varying *n*.

3.3 Reaction Products and Quantification

The thermogravimetric (TG) and differential thermogravimetric (DTG) curves of alkali activated slag pastes are shown in Figure 8. Figures 8(a) to (f) show the TG/DTG signatures of the pastes when activated using alkali silicate powder at n of 0.05 and varying M_s, or at M_s of 1.5 and 2.0 for varying *n*, after 28 days of curing. The main mass loss peak in the DTG curves in the 150°C-300°C region can be attributed to the major reaction product, C-A-S-H gel [44], which incorporates significant amounts of Al, depending on the reactive Al content of the slag [44-46]. When activators of high alkalinity are used, a more crystalline C-(N/K)-A-S-H gel has also been reported [47], where the alkali cations are also incorporated into the gel structure as charge balancers. These figures show that the total mass loss up to about 600°C, which is an indicator of the degree of reaction of these systems, is approximately the same at 28 days irrespective of the activator type. The 28-day DTG curves also show the presence of a hydrotalcite-like phase with a mass loss in the range of 300-400°C. Hydrotalcite phases have been commonly observed in alkali activated slag systems [45, 47-51] and they are found to increase with increasing reaction time. In the present study, product characterization has not been carried out beyond 28 days. The intensity of the C-(A)-S-H peak is similar for all the pastes after 28 days, for both sodium and potassium silicate activated mixtures. When the bound water contents (mass loss up to 600°C) were considered, no perceptible

differences were found between the Na- and K-silicate activated pastes (of the same activator M_s) cured for 28 days.

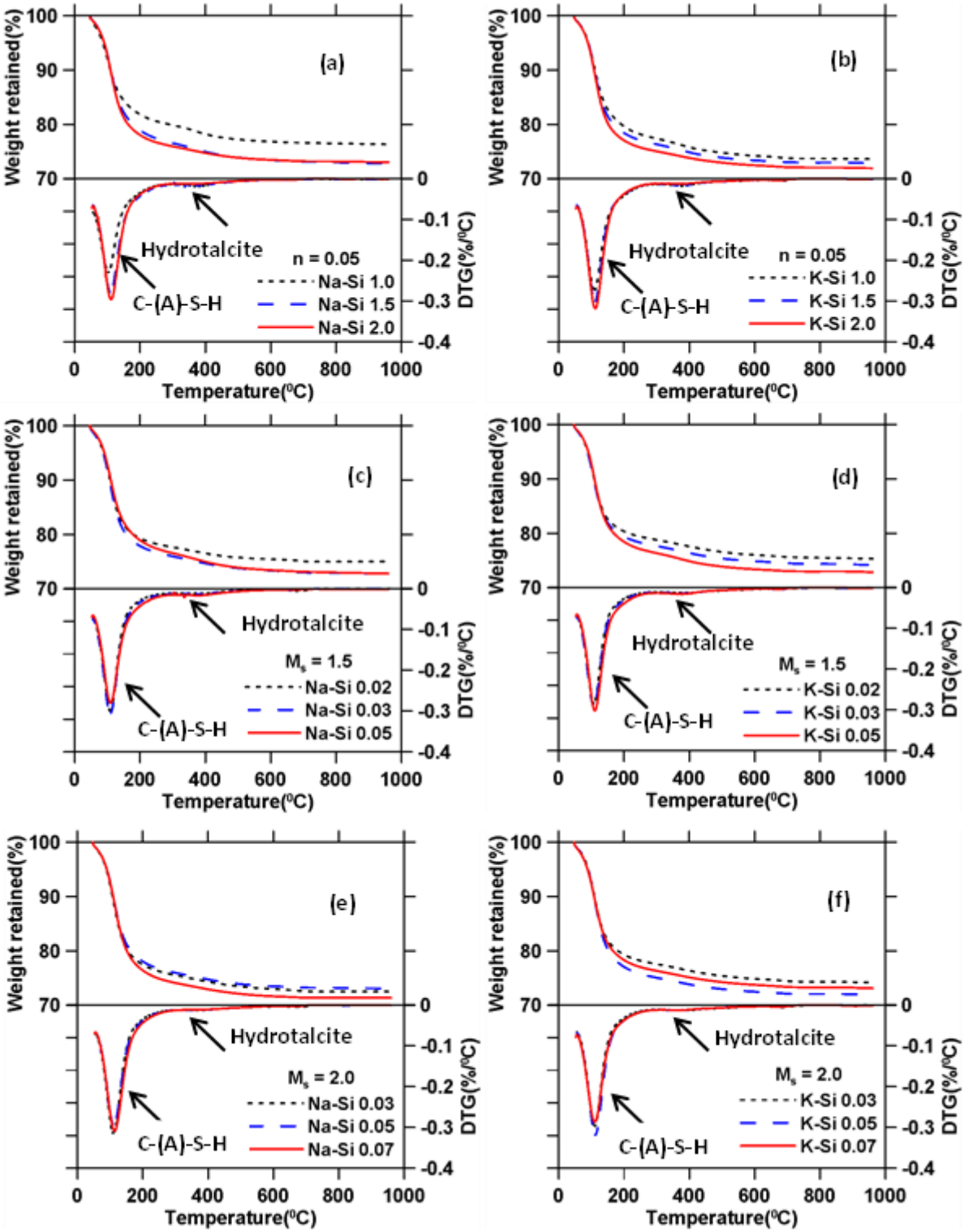

Figure 8 TG and DTG curves of Na-silicate and K-silicate activated slag pastes at 28 days: (a) and (b) n of 0.05 for different M_s, (c) and (d) M_s of 1.5 for different n, and (e) and (f) M_s of 2.0 for different n.

A quantification of the amount of C-A-S-H gel from TG data is generally difficult because the mass loss attributable to other reaction products such as hydrotalcite overlaps with that of C-A-S-H in the temperature range considered. However, it is possible to obtain a relative quantification of the amount of C-A-S-H gel since the other products are present only in very small amounts. Also, an assumption is made, quite appropriately, that the reaction product stoichiometry does not change significantly based on the type of alkali cation of the activator, or with the duration of reaction, especially after a significant amount of products are formed (say after 14 or 28 days). For example, when the Al/Si ratios of the reaction products were determined from ^{29}Si MAS NMR spectroscopy in our previous work where liquid activators were used [47], an Al/Si ratio of 0.12 was found for slag activated using an activator M_s of 1.5, and 0.11 when the M_s was increased to 2.0, irrespective of the alkali cation type. The Ca/Si ratio for the mixtures in this work was fixed at 0.80 based on past studies [45, 52] and the H/S ratio as 1.2 [53]. Figure 9 shows the relationship between the amounts of C-A-S-H gels obtained from TG/DTG analysis after 1, 7, and 28 days of reaction and the corresponding compressive strengths. The strength is found to be highly correlated to the amount of the gel, as expected, for both the Na- and K-silicate activated mixtures. It is well known that, in addition to the amount of C-A-S-H gel formed, the degree of polymerization of the gel, which depends on the alkali cation type and the silica modulus, also influences the strength [54]. The higher strength obtained for the K-silicate activated mortars even when the amount of gel formed is the same as that in Na-silicate activated mixtures, especially at later ages, point to a better polymerization in the former mixtures.

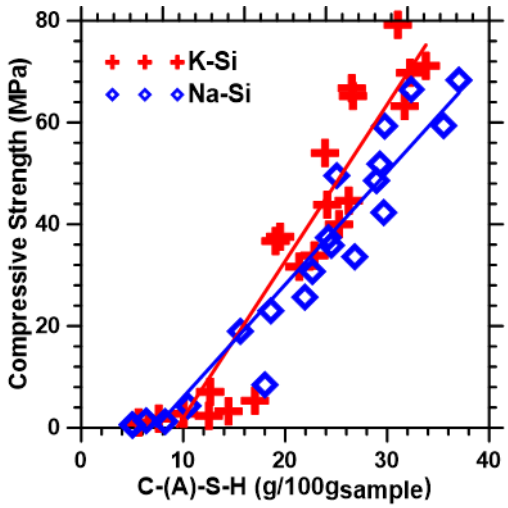

Figure 9 Variation of compressive strength of activated slag pastes as a function of the amount of C-A-S-H gel (g/100g of sample). The strength and C-A-S-H amounts at 1, 7, and 28 days are considered in this figure. The solid lines are to just guide the eye.

3.3 FTIR Spectroscopy

Figure 10 shows the FTIR Spectra of the sodium and potassium silicate powder activated slag pastes (a constant *n* value of 0.05 and varying M_s) after 1, 7, and 28 days of reaction. The small peaks corresponding to a wavenumber of around 1640 cm^{-1} is attributed to the OH group, which has relatively the same amplitude for all the pastes at all the ages. There is a small band associated with the stretching vibration of carbonate ions at around 1400 cm^{-1}; this can be ascribed to some amount

of carbonation that would have occurred during the mixing of the pastes. The major band appears in the 900-to-1000 cm^{-1} range, assigned to the vibration of Si-O-T (T being Si or Al) bonds [55-57], denoting the presence of C-A-S-H type gels. The widths of the band reduce over time, and the sharpness increases as the paste ages, showing that the polymerization degrees of the aluminosilicate groups have become more uniform. This can be noticed for both the Na-silicate (Figures 10 (a), (c), (e)) and K-silicate (Figures 10 (b), (d), (f)) activated pastes. The shoulder bands adjacent to the main peak, observed at a wavenumber range of 835-860 cm^{-1}, are representative of the symmetric and antisymmetric stretching of Si-O bonds, which are attributed to non-polymerized orthosilicate units from the unreacted slag [56]. Alkali activation results in silica polymerization and Al incorporation in the tetrahedra (with the alkali cations acting as charge balancers). This leads to a shift in the wavenumbers associated with the peaks and an increase in the amplitude of the Si-O-T antisymmetric stretching band with increasing in age, and with increase in M_s. With increasing time of reaction, the shoulder bands attributable to the unreacted slag also decreases in magnitude. When the FTIR spectra of Na- and K-silicate pastes are compared, the wavenumbers corresponding to the Si-O-T bonds are always found to be higher for the K-silicate activated pastes, at all ages. Higher wavenumbers indicate an enhanced degree of polymerization, and higher Al incorporation in the gel, which is attributable in part to the enhanced solubility of K-silicates in the alkaline solution [58]. Similar enhancements in wavenumbers for K-silicate liquid activated slag binders, when compared to Na-silicate liquid activated binders, have also been observed by the authors elsewhere [56]. A quantification of the Al incorporation in the gels with changes in n and M_s values or with reaction time is not attempted in this paper because the Si-O-Si and Si-O-Al bands share the same wavenumber range, necessitating NMR spectra to provide more clarity to this response.

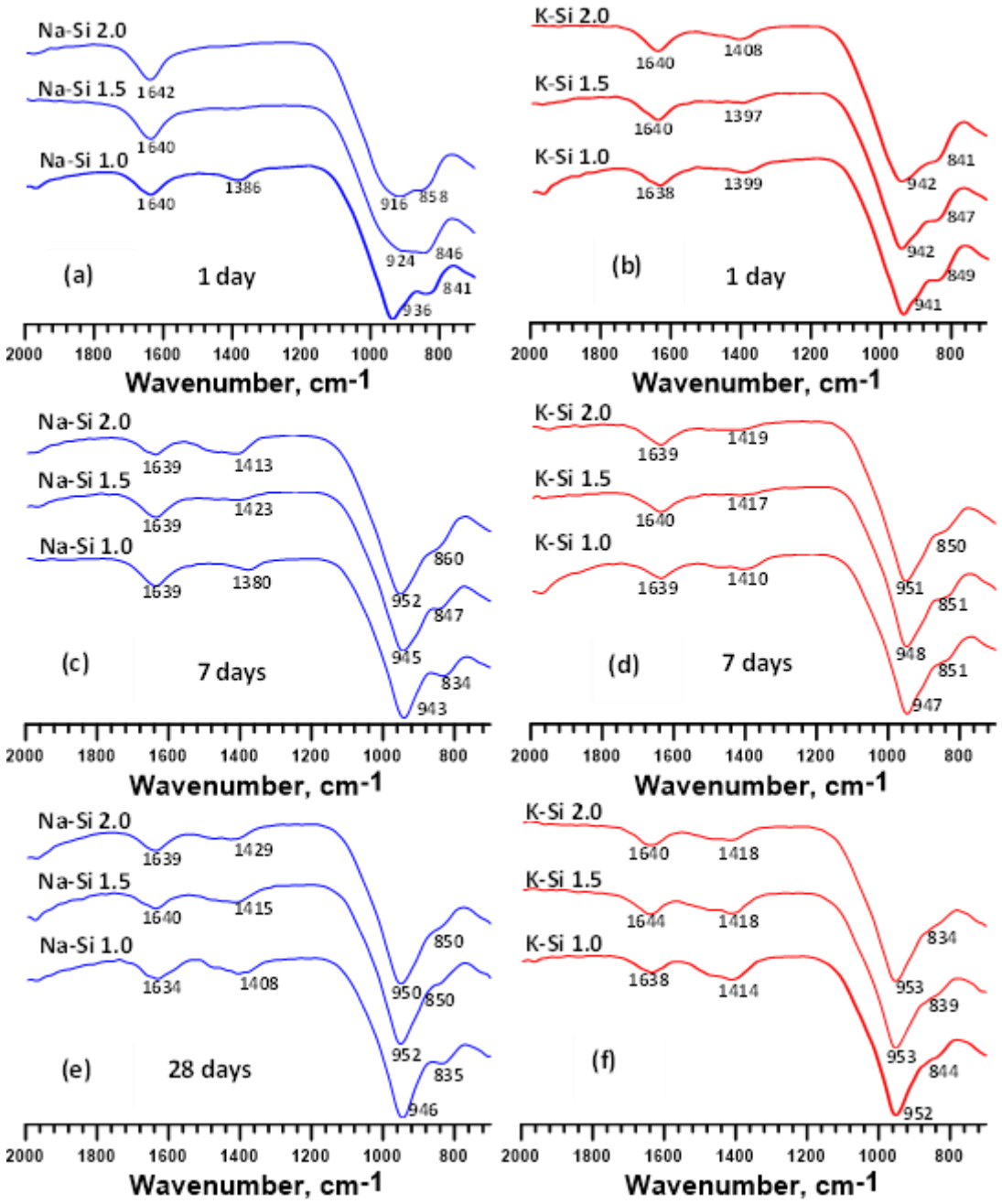

Figure 10 FTIR Spectra of Na-silicate pastes at: (a) 1 day, (c) 7 days, and (e) 28 days, and K-silicate pastes at: (b) 1 day, (d) 7 days, and (f) 28 days. The mixtures used an n value of 0.05 varying with M_s.

4. Conclusions

This paper has presented the results of experimental studies carried out with the aim of elucidating the influence of powder, "just-add-water" type activators on the reaction kinetics, compressive strength, and reaction product formation in alkali activated slag systems. Sodium and potassium silicates and hydroxides were used to provide the desired total alkalinity (*n*) and activator composition (silica-to-alkali oxide ratio, M_s) for the mixtures. The major conclusions are summarized in this section.

The heat evolution rates at early ages were found to be higher with decreasing activator M_s and increasing n for both the Na- and K-silicate activated pastes, but the trends were consistent for the K-silicate activated binders, owing to their enhanced solubility as compared to the Na-silicate activated pastes. The dormant period was much higher for Na-silicate activated pastes of higher M_s, but was relatively invariant to M_s (and chosen n values) for the K-silicate activated pastes, thus helping to choose the activator type based on desired setting times. Similar observations were noted in the compressive strength trends, where the strengths of the K-silicate activated systems were rather invariant with activator M_s, while significant differences existed in the strengths for Na-silicate activated mortars with respect to M_s. Higher later-age strengths for mixtures with a higher activator M_s points to the role of silicates in reaction product formation. This study also found that the influence of the cationic species was less important for later-age strengths at higher values of M_s, irrespective of the total alkalinity, n. This also underscores the importance of silicates from the activator in the strength development of alkali activated slag binders. The results showed that 28 to 56 day compressive strengths of 50-80 MPa can be obtained through proper selection of the activator type and alkalinity of the activation medium.

In general, higher later-age strengths were obtained for the K-silicate activated mortars at higher n value, which were corroborated with the approximate C-A-S-H gel amounts obtained from thermal analysis. The C-A-S-H gel amounts, varying from 5 g per 100 g of powder at early ages to 38 g/100 g of powder at later ages, scaled well with the compressive strengths. For the same amount of C-A-S-H gel, the K-silicate activated binders showed higher strengths, indicating that there are differences in the degree of polymerization of the reaction product. This was confirmed using FTIR spectra of Na- and K-silicate pastes where the wavenumbers corresponding to the Si-O-T bonds were found to be higher for the K-silicate activated pastes at all ages, which denoted an enhanced degree of polymerization and higher Al incorporation in the gel. This work thus has demonstrated the significant reaction rate, strength, and reaction product composition aspects that are critical to the use of “just-add-water” type activators in the development of sustainable, cement-less binder systems for concrete.

Acknowledgments

The authors gratefully acknowledge Holcim US and PQ Corporation for providing the materials used in this study. The work was carried out in the Laboratory for the Science and Sustainable Infrastructural Materials (LS-SIM) at Arizona State University, and the support that has made the establishment and operation of these laboratories are also acknowledged.

Author Contributions

Akash Dakhane is responsible for the experiments and data collection, while Narayanan Neithalath procured funding, oversaw the research, and prepared the manuscript.

Competing Interests

The authors have declared that no competing interests exist.

References

1. Habert G, d'Espinose de Lacaillerie JB, Roussel N. An environmental evaluation of geopolymer based concrete production: Reviewing current research trends. J Clean Prod. 2011; 19: 1229-1238.
2. Lolli F, Kurtis KE. Life Cycle Assessment of alkali activated materials: Preliminary investigation for pavement applications. RILEM Tech Lett. 2021; 6: 124-130.
3. Mellado A, Catalán C, Bouzón N, Borrachero MV, Monzó JM, Payá J. Carbon footprint of geopolymeric mortar: Study of the contribution of the alkaline activating solution and assessment of an alternative route. RSC Adv. 2014; 4: 23846-23852.
4. Roy DM. Alkali-activated cements opportunities and challenges. Cem Concr Res. 1999; 29: 249-254.
5. Palomo A, Grutzeck MW, Blanco MT. Alkali-activated fly ashes: A cement for the future. Cem Concr Res. 1999; 29: 1323-1329.
6. Xu H, Van Deventer JSJ. The geopolymerisation of alumino-silicate minerals. Int J Miner Process. 2000; 59: 247-266.
7. Bijen J. Benefits of slag and fly ash. Constr Build Mater. 1996; 10: 309-314.
8. Bernal SA, Mejía de Gutiérrez R, Provis JL. Engineering and durability properties of concretes based on alkali-activated granulated blast furnace slag/metakaolin blends. Constr Build Mater. 2012; 33: 99-108.
9. Fernandez Jimenez A, García-Lodeiro I, Palomo A. Durability of alkali-activated fly ash cementitious materials. J Mater Sci. 2007; 42: 3055-3065.
10. Abdollahnejad Z, Mastali M, Falah M, Shaad KM, Luukkonen T, Illikainen M. Durability of the reinforced one-part alkali-activated slag mortars with different fibers. Waste Biomass Valorization. 2021; 12: 487-501.
11. Vance K, Aguayo M, Dakhane A, Ravikumar D, Jain J, Neithalath N. Microstructural, mechanical, and durability related similarities in concretes based on OPC and alkali-activated slag binders. Int J Concr Struct Mater. 2014; 8: 289-299.
12. Marathe S, Mithanthaya IR, Shenoy RY. Durability and microstructure studies on Slag-Fly Ash-Glass powder based alkali activated pavement quality concrete mixes. Constr Build Mater. 2021; 287: 123047.
13. Ibrahim M, Maslehuddin M. An overview of factors influencing the properties of alkali-activated binders. J Clean Prod. 2021; 286: 124972.
14. Chithiraputhiran S, Neithalath N. Isothermal reaction kinetics and temperature dependence of alkali activation of slag, fly ash and their blends. Constr Build Mater. 2013; 45: 233-242.
15. Elahi MMA, Hossain MM, Karim MR, Zain MFM, Shearer C. A review on alkali-activated binders: Materials composition and fresh properties of concrete. Constr Build Mater. 2020; 260: 119788.
16. Tänzer R, Buchwald A, Stephan D. Effect of slag chemistry on the hydration of alkali-activated blast-furnace slag. Mater Struct. 2015; 48: 629-641.
17. Perumal P, Sreenivasan H, Luukkonen T, Kantola AM, Telkki VV, Kinnunen P, et al. High strength one-part alkali-activated slag blends designed by particle packing optimization. Constr Build Mater. 2021; 299: 124004.
18. Lima FS, Gomes TCF, de Moraes JCB. Novel one-part alkali-activated binder produced with coffee husk ash. Mater Lett. 2022; 313: 131733.

19. Luukkonen T, Abdollahnejad Z, Yliniemi J, Kinnunen P, Illikainen M. One-part alkali-activated materials: A review. Cem Concr Res. 2018; 103: 21-34.
20. Neupane K. "Fly ash and GGBFS based powder-activated geopolymer binders: A viable sustainable alternative of portland cement in concrete industry." Mech Mater. 2016; 103: 110-122.
21. Neupane K. High-strength geopolymer concrete- properties, advantages and challenges. Adv Mater. 2018; 7: 15-25.
22. Yang KH, Song JK, Ashour AF, Lee ET. Properties of cementless mortars activated by sodium silicate. Constr Build Mater. 2008; 22: 1981-1989.
23. Nematollahi B, Sanjayan J, Shaikh FUA. Synthesis of heat and ambient cured one-part geopolymer mixes with different grades of sodium silicate. Ceram Int. 2015; 41: 5696-5704.
24. Hajimohammadi A, van Deventer JSJ. Characterisation of one-part geopolymer binders made from fly ash. Waste Biomass Valorization. 2017; 8: 225-233.
25. Peys A, Rahier H, Pontikes Y. Potassium-rich biomass ashes as activators in metakaolin-based inorganic polymers. Appl Clay Sci. 2016; 119: 401-409.
26. Hajimohammadi A, van Deventer JSJ. Solid reactant-based geopolymers from rice hull ash and sodium aluminate. Waste Biomass Valorization. 2017; 8: 2131-2140.
27. Nematollahi B, Sanjayan J, Qiu J, Yang EH. Micromechanics-based investigation of a sustainable ambient temperature cured one-part strain hardening geopolymer composite. Constr Build Mater. 2017; 131: 552-563.
28. Kim MS, Jun Y, Lee C, Oh JE. Use of CaO as an activator for producing a price-competitive non-cement structural binder using ground granulated blast furnace slag. Cem Concr Res. 2013; 54: 208-214.
29. Garg N, White CE. Mechanism of zinc oxide retardation in alkali-activated materials: An in situ X-ray pair distribution function investigation. J Mater Chem A. 2017; 5: 11794-11801.
30. Brough AR, Holloway M, Sykes J, Atkinson A. Sodium silicate-based alkali-activated slag mortars Part II. The retarding effect of additions of sodium chloride or malic acid. Cem Concr Res. 2000; 30: 1375-1379.
31. Ravikumar D, Neithalath N. Effects of activator characteristics on the reaction product formation in slag binders activated using alkali silicate powder and NaOH. Cem Concr Compos. 2012; 34: 809-818.
32. Ravikumar D, Neithalath N. Reaction kinetics in sodium silicate powder and liquid activated slag binders evaluated using isothermal calorimetry. Thermochim Acta. 2012; 546: 32-43.
33. Chithiraputhiran SR. Kinetics of alkaline activation of slag and fly ash-slag systems. Arizona: Arizona State University: 2012.
34. C09 Committee. Practice for Measuring Hydration Kinetics of Hydraulic Cementitious Mixtures Using Isothermal Calorimetry [Internet]. ASTM International. 2009. [cited date 2013 October 19]. Available from: http://enterprise.astm.org.ezproxy1.lib.asu.edu/.
35. Barbosa VFF, MacKenzie KJD. Thermal behaviour of inorganic geopolymers and composites derived from sodium polysialate. Mater Res Bull. 2003; 38: 319-331.
36. Duxson P, Lukey GC, van Deventer JSJ. Physical evolution of Na-geopolymer derived from metakaolin up to 1000 °C. J Mater Sci. 2007; 42: 3044-3054.
37. Duxson P, Lukey GC, van Deventer JSJ. The thermal evolution of metakaolin geopolymers: Part 2 - Phase stability and structural development. J Non-Cryst Solids. 2007; 353: 2186-2200.

38. Bach TTH, Chabas E, Pochard I, Cau Dit Coumes C, Haas J, Frizon F, et al. Retention of alkali ions by hydrated low-pH cements: Mechanism and Na^+/K^+ selectivity. Cem Concr Res. 2013; 51: 14-21.
39. Provis JL, van Deventer JSJ. Geopolymerisation kinetics. 1. In situ energy-dispersive X-ray diffractometry. Chem Eng Sci. 2007; 62: 2309-2317.
40. Khale D, Chaudhary R. Mechanism of geopolymerization and factors influencing its development: A review. J Mater Sci. 2007; 42: 729-746.
41. Phair JW, Van Deventer JSJ. Effect of the silicate activator pH on the microstructural characteristics of waste-based geopolymers. Int J Miner Process. 2002; 66: 121-143.
42. Shi C, Day RL. A calorimetric study of early hydration of alkali-slag cements. Cem Concr Res. 1995; 25: 1333-1346.
43. Shi C, Day RL. Some factors affecting early hydration of alkali-slag cements. Cem Concr Res. 1996; 26: 439-447.
44. Schneider J, Cincotto MA, Panepucci H. 29Si and 27Al high-resolution NMR characterization of calcium silicate hydrate phases in activated blast-furnace slag pastes. Cem Concr Res. 2001; 31: 993-1001.
45. Lothenbach B, Gruskovnjak A. Hydration of alkali-activated slag: Thermodynamic modelling. Adv Cem Res. 2007; 19: 81-92.
46. Wang SD, Scrivener KL. 29Si and 27Al NMR study of alkali-activated slag. Cem Concr Res. 2003; 33: 769-774.
47. Haha MB, Le Saout G, Winnefeld F, Lothenbach B. Influence of activator type on hydration kinetics, hydrate assemblage and microstructural development of alkali activated blast-furnace slags. Cem Concr Res. 2011; 41: 301-310.
48. Haha MB, Lothenbach B, Le Saout G, Winnefeld F. Influence of slag chemistry on the hydration of alkali-activated blast-furnace slag - Part II: Effect of Al_2O_3. Cem Concr Res. 2012; 42: 74-83.
49. Puertas F, Fernández Jiménez A. Mineralogical and microstructural characterisation of alkali-activated fly ash/slag pastes. Cem Concr Compos. 2003; 25: 287-292.
50. Brew DMR, Glasser FP. The magnesia-silica gel phase in slag cements: Alkali (K, Cs) sorption potential of synthetic gels. Cem Concr Res. 2005; 35: 77-83.
51. Wang SD, Scrivener KL. Hydration products of alkali activated slag cement. Cem Concr Res. 1995; 25: 561-571.
52. Fernández Jiménez A, Zibouche F, Boudissa N, García Lodeiro I, Abadlia MT, Palomo A. "Metakaolin-slag-clinker blends." The role of Na^+ or K^+ as alkaline activators of theses ternary blends. J Am Ceram Soc. 2013; 96: 1991-1998.
53. Chen W, Brouwers HJH. The hydration of slag, part 1: Reaction models for alkali-activated slag. J Mater Sci. 2007; 42: 428-443.
54. Dakhane A. Multiscale engineering response of alkali activated aluminosilicate binders. Arizona: Arizona State University; 2016.
55. Madavarapu SB. FTIR analysis of alkali activated slag and fly ash using deconvolution techniques Arizona: Arizona State University; 2014
56. Dakhane A, Madavarapu SB, Marzke R, Neithalath N. Time, temperature, and cationic dependence of alkali activation of slag: Insights from fourier transform infrared spectroscopy and spectral deconvolution. Appl Spectrosc. 2017; 71: 1795-1807.

57. Lee WKW, van Deventer JSJ. Use of infrared spectroscopy to study geopolymerization of heterogeneous amorphous aluminosilicates. Langmuir. 2003; 19: 8726-8734.
58. Walkley B, Ke X, Provis JL, Bernal SA. Activator anion influences the nanostructure of alkali-activated slag cements. J Phys Chem C. 2021; 125: 20727-20739.